(iii) When $[Co(Pypep)_2]^+$ is reduced electrochemically, an unstable cobalt(II) species is formed. Rapid ligand reorganization in the first coordination sphere of the Co(II) center of this intermediate results in a high-spin octahedral cobalt(II) complex that can be independently synthesized by mixing cobalt(II) acetate and **1** (ratio 1:2) in degassed methanol.

(iv) The solution structure of the cobalt(III) complex has been proposed on the basis of one- and two-dimensional NMR data. Similar experiments with partially hydrolyzed Co(III)-BLM are expected to provide valuable information regarding the coordination structure of Co(III)-BLM.

Acknowledgment. This research was supported by a Faculty Research Grant and the donors of the Petroleum Research Fund, administered by the American Chemical Society, at the University of California and by NIH Grant GM 32690 at the University of Texas. We thank S. Brown for help in the synthesis of PypepH. Experimental assistance from S. Hudson and J. Loo is gratefully acknowledged.

Registry No. **2**, 112247-29-7; $[Co(Pypep)_2]ClO_4$, 112247-28-6; $[Co(Pypep)_2]BF_4$, 112247-30-0.

Supplementary Material Available: Crystal structure data for $[Co(Pypep)_2]ClO_4 \cdot H_2O$ (**2**) including thermal parameters for non-hydrogen atoms (Table S1), bond distances and angles in the anion (Table S2), positional parameters for the hydrogen atoms (Table S3), and unweighted least-squares planes of the cation (Table S4) and NMR data for **2** including coupling constants for the CH_2 protons of the ligand (Table S6) and the long-range (J = 9 Hz) ^1H-^{13}C COSY spectrum of **2** in Me_2SO-d_6 (Figure S1) (9 pages); observed and calculated structure factors (Table S5) (11 pages). Ordering information is given on any current masthead page.

Contribution from the Division of Chemical and Physical Sciences, Deakin University, Waurn Ponds 3217, Victoria, Australia, and Department of Inorganic Chemistry, University of Melbourne, Parkville 3052, Victoria, Australia

Electrochemical Reduction and Oxidation in Noncoordinating and Coordinating Solvents of Two Closely Related Binuclear Nickel(II) Complexes Containing either Sulfur or Oxygen Endogenous Bridging Centers

Alan M. Bond,*[1] Masa-aki Haga,[1,2] Ian S. Creece,[1] Richard Robson,[3] and Jenny C. Wilson[3]

Received April 27, 1987

Replacement of oxygen by sulfur as the endogenous bridging center of the nickel binuclear complexes $L(X)Ni_2(pz)$ (X = O, S; pz = pyrazolate; L = binucleating ligand component with peripheral *tert*-butyl substituents to solubilize the complexes in nonpolar solvents) leads to remarkable differences in their solution and redox chemistry. Whereas the diamagnetic planar complex $L(S)Ni_2(pz)$ shows no detectable specific solvent interaction in coordinating solvents such as dimethylformamide (DMF), the oxygen analogue forms the paramagnetic species $L(O)Ni_2(pz)(DMF)_2$ in solution from which the solid monosolvate $L(O)Ni_2(pz)(DMF)$ can be isolated. The reversible half-wave potentials, $E_{1/2}^r$, for the reduction processes

$$L(S)Ni_2(pz) \underset{-e^-}{\overset{+e^-}{\rightleftharpoons}} [L(S)Ni_2(pz)]^- \underset{-e^-}{\overset{+e^-}{\rightleftharpoons}} [L(S)Ni_2(pz)]^{2-}$$

as measured by voltammetric studies at platinum, gold, glassy-carbon, and mercury electrodes are separated by several hundred millivolts. In the noncoordinating nonpolar solvent dichloromethane, the reduced binuclear complexes are highly reactive. Nonspecific effects in polar solvents provide stability in the kinetic sense, whereas thermodynamic redox potentials are essentially solvent independent. By contrast, the two oxidation processes

$$L(S)Ni_2(pz) \underset{+e^-}{\overset{-e^-}{\rightleftharpoons}} [L(S)Ni_2(pz)]^+ \underset{+e^-}{\overset{-e^-}{\rightleftharpoons}} [L(S)Ni_2(pz)]^{2+}$$

have similar $E_{1/2}^r$ values and exhibit substantial specific solvent effects as does a further two-electron process to generate a highly reactive formally nickel(IV) complex $[L(S)Ni_2(pz)]^{4+}$. The solvent dependence of the cyclic voltammetry of the $L(O)Ni_2(pz)$ complex is substantially more complex than that for the sulfur analogue. Temperature and scan rate dependence as well as the presence of additional processes are observed in coordinating solvents that reflect the strong specific solvation terms associated with the coexistence of a range of $[L(O)Ni_2(pz)(solvent)_n]^m$ complexes (n = 0-4, m = 2+/+/0/-/2-) in coordinating solvents. Since the majority of voltammetric studies on nickel binuclear complexes have been conducted in solvents such as dimethylformamide or acetonitrile, the present information can be used to rationalize unexplained complexities previously reported on this important class of binuclear complex. Interestingly, the sulfur binuclear complex is more difficult to oxidize than the oxygen analogue, which is contrary to normal expectations. This illustrates the importance of the nature of the endogenous bridging centers in binuclear complexes.

Introduction

There has been extensive interest in the redox properties of binuclear transition-metal complexes of the type M_2L (M = metal, L = binucleating ligand(s)), particularly where M is copper or nickel. Binuclear complexes of this kind are of interest because the redox properties may be related to the multinuclear metal sites in metalloproteins,[4] particularly binuclear type III copper proteins.[5,6]

The majority of electrochemical studies on Cu_2L and Ni_2L complexes simply have reported half-wave potentials and whether the reduction and oxidation processes are reversible or irreversible. Furthermore, for reasons of solubility, almost all studies have been confined to coordinating solvents such as dimethylformamide (DMF) or acetonitrile (CH_3CN).[7-21] However, detailed elec-

(1) Deakin University.
(2) On leave from Mie University, Tsu, Mie, Japan.
(3) University of Melbourne.
(4) Sadler, P. J. *Inorg. Perspect. Biol. Med.* **1978**, *1*, 233.
(5) (a) Beinert, H. *Coord. Chem. Rev.* **1980**, *33*, 55. (b) Karlin, K. D.; Gultneh, Y. *J. Chem. Educ.* **1985**, *62*, 983.
(6) (a) *Copper Proteins and Copper Enzymes*; Lontie, R., Ed.; CRC: Boca Raton, FL, 1984, Vols. 1-3. (b) Solomon, E. D. *Copper Proteins*; Spiro, T. G. Ed.; Wiley: New York 1981; Chapter 2 and references therein.
(7) (a) Mazurek, W.; Bond, A. M.; O'Connor, M. J.; Wedd, A. G. *Inorg. Chem.* **1986**, *25*, 906 and references cited therein. (b) Nag, K.; Chakravorty, A. *Coord. Chem. Rev.* **1980**, *33*, 87. (c) Haines, R. I.; McAuley, A. *Coord. Chem. Rev.* **1981**, *39*, 77. (d) Addison, A. W. *Inorg. Nucl. Chem. Lett.* **1976**, *12*, 899. (e) Lintvedt, R. L.; Ranger, G.; Kramer, L. S. *Inorg. Chem.* **1986**, *25*, 2635.

0020-1669/88/1327-0712$01.50/0 © 1988 American Chemical Society

trochemical investigations[7-11] have revealed that the nature of (i) the electrolyte, (ii) the electrode, (iii) the flexibility or otherwise of endogenous and exogenous bridges, and (iv) the solvent can make substantial differences to the redox chemistry and need to be considered in any detailed discussion of electron-transfer reactions associated with binuclear complexes.

In the present paper an extensive electrochemical investigation is presented on the nickel(II) complexes IA and IB, which differ

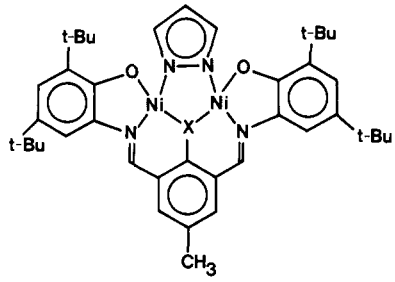

IA ; X = S
IB ; X = O

only in the endogenous bridging atom (sulfur in the former case, oxygen in the latter). The binucleating ligand component of IA will be represented below as $L(S)^{3-}$ and that of IB as $L(O)^{3-}$ so that IA will be referred to as $L(S)Ni_2(pz)$ and IB as $L(O)Ni_2(pz)$ where pz symbolizes the coordinated pyrazolate. In contrast to the insoluble complexes previously synthesized from binucleating ligands with side arms derived from unsubstituted *o*-aminophenol,[22a] the present complexes, with four peripheral *tert*-butyl substituents, are sufficiently soluble to allow physical studies in a range of solvents including nonpolar, noncoordinating solvents such as dichloromethane. The present matched pair of complexes therefore provides a unique opportunity to study the role of the solvent as well as the influence on redox properties introduced by changing the endogenous bridging center from oxygen to sulfur. Importantly, the influence of a range of parameters on both reduction and oxidation processes can be studied in detail, in contrast to the majority of previous studies where investigations were confined to either reduction or oxidation.

Experimental Section

Synthesis. $L(S)Ni_2(pz)$. To a solution of 2-amino-4,6-di-*tert*-butylphenol (2.63 g, 11.9 mmol) in methanol (45 cm^3) was added 2-((*N*,*N*-dimethylcarbamoyl)thio)-5-methylisophthalaldehyde (1.36 g, 5.4 mmol) in boiling methanol (50 cm^3). The resulting orange solution was heated under reflux for 10 min and then allowed to cool to room temperature. The fine yellow needles of the (dimethylcarbamoyl)sulfur-protected ligand were collected, washed with methanol, and dried in vacuo. Yield: 2.63 g, 74%. A mixture of this sulfur-protected ligand (0.31 g, 0.47 mmol) and pyrazole (0.05 g, 0.79 mmol) in chloroform (3 cm^3) was added to a filtered solution of nickel(II) acetate tetrahydrate (0.24 g, 0.96 mmol) in boiling methanol (10 cm^3). The resulting homogeneous solution was heated under reflux for 30 min during which time crystalline $L(S)Ni_2(pz)$ separated. The crystals were collected, washed with methanol, and dried in vacuo at 80 °C. Yield: 0.25 g, 71%. Anal. Calcd for $C_{40}H_{50}N_4O_2SNi_2$: C, 62.5; H, 6.6; N, 7.3. Found: C, 62.7; H, 6.1; N, 7.2.

$L(O)Ni_2(pz)$. 2-Hydroxy-5-methylisophthalaldehyde (0.88 g, 5.39 mmol) in boiling methanol (20 cm^3) was added to a boiling solution of 2-amino-4,6-di-*tert*-butylphenol (3.0 g, 13.6 mmol) in methanol (45 cm^3). The red solution so formed was heated under reflux for 10 min during which time orange needles of the phenolic di-Schiff-base ligand, $L(O)H_3$, separated. The solid was collected, washed with methanol, and dried at 80 °C in vacuo. Yield: 82%. To a filtered solution of nickel(II) acetate tetrahydrate (0.094 g, 0.38 mmol) in boiling methanol (4 cm^3) was added a solution of $L(O)H_3$ (0.089 g, 0.16 mmol) and pyrazole (0.026 g, 0.41 mmol) in chloroform (1 cm^3). The mixture was heated under reflux for 30 min, during which time crystalline $L(O)Ni_2(pz)$ separated. After the mixture had cooled to room temperature, the $L(O)Ni_2(pz)$ was collected, washed with methanol, and dried in vacuo at 80 °C. Yield: 93%. Anal. Calcd for $C_{40}H_{50}N_4O_3Ni_2$: C, 63.9; H, 6.7; H, 7.4. Found: C, 64.0; H, 6.8; N, 7.3.

Solvents and Electrolytes for Electrochemical Measurements. Dichloromethane was of HPLC grade and dried with A4 molecular sieves. Acetone was dried over Drierite (calcium sulfate). Tetrahydrofuran (THF) was dried over lithium aluminum hydride, and propyl cyanide (PrCN), which is also commonly referred to as butyronitrile or butanenitrile, was dried over phosphorus pentoxide. Dimethylformamide (DMF) was allowed to stand over alumina for 24 h, decanted, and distilled in vacuo prior to use. All purified solvents were stored under nitrogen over 4A molecular sieves. Tetrabutylammonium perchlorate (Bu_4NClO_4), tetraethylammonium perchlorate (Et_4NClO_4), tetrabutylammonium tetrafluoroborate (Bu_4NBF_4), and tetrabutylammonium hexafluorophosphate (Bu_4NPF_6) were purchased from Southwestern Analytical Chemicals, Inc. (Austin, TX), and dried in vacuo at 70 °C for 12 h.

Physical Measurements. Electronic spectra were recorded on a Hitachi U-3200 spectrophotometer using 1-cm matched quartz cells. Spectrophotometric titrations with DMF were performed in CH_2Cl_2 solutions. The concentration of binuclear compound was kept constant at 6×10^{-4} M, and the added concentration range of DMF was 0.4–4 M. The spectral data were analyzed by using the following equation:[23] $\log [(A_{obsd} - A_0)/(A_\infty - A_{obsd})] = n \log [DMF] + \log K$, where A_{obsd} = the absorbance observed at a given wavelength, A_0 = the initial absorbance, and A_∞ = the final absorbance. The values for equilibrium constant, K, and the number of coordinated DMF ligands bound in a complex, n, were obtained from a plot of $\log [(A_{obsd} - A_0)/A_\infty - A_{obsd})]$ vs log [DMF].

Magnetic moments were measured by the Gouy method. Proton NMR spectra were recorded with a JEOL FX100 spectrometer using tetramethylsilane (TMS) as an internal reference. Analyses were performed by Amdel, Australian Microanalytical Service, Melbourne, Australia.

Electrochemical measurements (cyclic voltammetry and hydrodynamic voltammetry) were performed with a BAS-100 electrochemical analyzer or a Princeton Applied Research (PAR) Model 174 polarographic analyzer connected to a Houston Instruments 2000 X-Y recorder. The working electrodes were platinum disk (Pt), glassy-carbon disk (GC), gold disk (Au), and hanging mercury drop (Hg). A platinum-wire auxiliary electrode was used, and a reference electrode, Ag/AgCl (saturated LiCl in acetone), was separated from the test solution by a salt bridge containing the same solvent and supporting electrolyte used in the test solution. The ferrocene-ferrocenium (Fc/Fc^+) oxidation process was used as an internal standard and all potentials were referred to this standard reference system. A Metrohm rotating disk electrode assembly Model 628-10 was used for the hydrodynamic voltammetry. Coulometry was undertaken by using a PAR Model 173 potentiostat and a PAR Model 179 digital coulometer at a platinum-gauze working electrode. The reference electrode was the same Ag/AgCl electrode used in voltammetric experiments and the auxiliary electrode was platinum gauze separated from the test solution by a salt bridge containing the solvent mixture.

Results and Discussion

$L(S)Ni_2(pz)$. (a) Reduction of $L(S)Ni_2(pz)$ in CH_2Cl_2. Figure 1 shows that two well-separated reduction steps are observed for $L(S)Ni_2(pz)$ in CH_2Cl_2 under conditions of cyclic voltammetry and differential-pulse voltammetry. The two processes are labeled

(8) Lintvedt, R. L.; Kramer, L. S. *Inorg. Chem.* **1983**, *22*, 796.
(9) Lintvedt, R. L.; Kramer, L. S.; Ranger, G.; Corfield, P. W.; Glick, M. D. *Inorg. Chem.* **1983**, *22*, 3580.
(10) Meyer, G.; Nadjo, L.; Lapinte, C. *Nouv. J. Chim.* **1984**, *8*, 777.
(11) Mazurek, W.; Bond, A. M.; Murray, K. S.; O'Connor, M. J.; Wedd, A. G. *Inorg. Chem.* **1985**, *24*, 2484.
(12) Gagné, R. R.; Koval, C. A.; Smith, T. J.; Cimolino, M. C. *J. Am. Chem. Soc.* **1979**, *101*, 4571.
(13) Gagné, R. L.; Spiro, C. L. *J. Am. Chem. Soc.* **1980**, *102*, 1443.
(14) Gagné, R. R.; Henling, L. M.; Kistenmacher, T. J. *Inorg. Chem.* **1980**, *19*, 1226.
(15) Long, R. C.; Hendrickson, D. N. *J. Am. Chem. Soc.* **1983**, *105*, 1513.
(16) Drago, R. S.; Desmond, M. J.; Corden, B. B.; Miller, K. A. *J. Am. Chem. Soc.* **1983**, *105*, 2287.
(17) Gisselbrecht, J.-P.; Gross, M.; Lehn, J.-M.; Sauvage, J.-P.; Ziessel, R.; Piccinni-Leopardi, C.; Arrieta, J. M.; Germain, G.; Meerssche, M. V. *Nouv. J. Chim.* **1984**, *8*, 661.
(18) Latour, J.-M.; Limosin, D.; Rey, P. *J. Chem. Soc., Chem. Commun.* **1985**, 464.
(19) Acholla, F. V.; Takusagawa, F.; Mertes, K. B. *J. Am. Chem. Soc.* **1985**, *107*, 6902.
(20) Geiger, W. E. *Prog. Inorg. Chem.* **1985**, *33*, 275.
(21) Hartman, J. R.; Cooper, S. R. *J. Am. Chem. Soc.* **1986**, *108*, 1202.
(22) (a) Hughes, J. G.; Robson, R. *Inorg. Chim. Acta* **1979**, *35*, 87. (b) Robson, R. *Inorg. Nucl. Chem. Lett.* **1970**, *6*, 125. (c) McFadyen, W. D.; Robson, R.; Schaap, H. A. *J. Coord. Chem.* **1978**, *8*, 59.
(23) Rillema, D. P.; Wicker, C. M., Jr.; Morgan, R. D.; Barringer, L. F.; Scism, L. A. *J. Am. Chem. Soc.* **1982**, *104*, 1276.

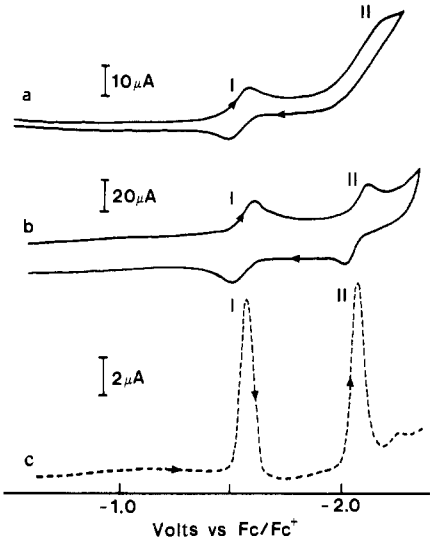

Figure 1. Cyclic voltammograms (a, b) and a differential-pulse voltammogram (c) for the reduction of $L(S)Ni_2(pz)$ in CH_2Cl_2 (0.1 M Bu_4NClO_4) at a glassy-carbon electrode: (a) $T = 20$ °C, scan rate = 100 mV s^{-1}; (b) $T = -70$ °C, scan rate = 1 V s^{-1}; (c) $T = -70$ °C, scan rate = 4 mV s^{-1}, pulse amplitude = −50 mV, pulse width = 60 ms, duration between pulses = 1 s.

I and II. Cyclic voltammetric data (Figure 1a) at scan rates >100 mV s^{-1} and at 20 °C are consistent with process 1 being assigned to the chemically reversible process

$$L(S)Ni_2(pz) + e^- \rightleftharpoons [L(S)Ni_2(pz)]^- \quad (1)$$

At low scan rates (20 mV s^{-1}), some chemical irreversibility is observed, suggesting that the $[L(S)Ni_2(pz)]^-$ species is not likely to be stable in CH_2Cl_2 on the synthetic time scale. The limiting current per unit concentration for process I at a rotating disk electrode is the same (except for sign) as that in processes III and IV (see later) confirming that this is a one-electron-transfer process.

Process II is a multielectron process at 20 °C (Figure 1a). At fast scan rates (>1 V s^{-1}) and low temperature (−70 °C), process II becomes a chemically reversible electron process (Figure 1b), which involves transfer of one electron, as evidenced by the magnitude of differential-pulse peak heights and shapes relative to those of process I (Figure 1c). At −70 °C, process II is the simple reaction

$$[L(S)Ni_2(pz)]^- + e^- \rightleftharpoons [L(S)Ni_2(pz)]^{2-} \quad (2)$$

Low-temperature data enables the separation in reversible half-wave potential $(\Delta E_{1/2}{}^r)_{I,II}{}^{red}$ to be calculated as 0.55 V. Decomposition of $[L(S)Ni_2(pz)]^{2-}$, releasing reducible free ligand(s) (e.g. double bonds), and/or reduction of formally nickel(I) species to nickel(0) would lead to the observation of a multielectron response for process II at room temperature. In the noncoordinating solvent dichloromethane, the formally d^9 $[L(S)Ni_2(pz)]^{2-}$ binuclear complex is highly reactive and even less amenable to isolation than $[L(S)Ni_2(pz)]^-$.

Table I includes data for reduction of $L(S)Ni_2(pz)$ at Pt, GC, Au, and Hg electrodes in dichloromethane and it can be noted that processes I and II are independent of electrode material within experimental error.

(b) Oxidation of $L(S)Ni_2(pz)$ in CH_2Cl_2. Figure 2a is a cyclic voltammogram for oxidation of $L(S)Ni_2(pz)$ in CH_2Cl_2 at a glassy-carbon electrode. Three well-defined oxidation processes, III, IV, and V, are observed. When the potential is switched at +0.8 V vs Fc/Fc^+, two chemically reversible one-electron-oxidation processes (scan rates 20–500 mV s^{-1}) having the same current per unit concentration values as reduction process I are found. Processes III and IV can therefore be assigned to the electrode reactions

$$L(S)Ni_2(pz) \rightleftharpoons [L(S)Ni_2(pz)]^+ + e^- \quad (3)$$

$$[L(S)Ni_2(pz)]^+ \rightleftharpoons [L(S)Ni_2(pz)]^{2+} + e^- \quad (4)$$

Table I. Cyclic Voltammetric Data[a] for Reduction and Oxidation of $L(S)Ni_2(pz)$ in CH_2Cl_2 (0.1 M Bu_4NClO_4) at 20 °C Using a Scan Rate of 100 mV s^{-1}

electrode	process		E_p, V vs Fc/Fc^+	ΔE_p, mV	$E_{1/2}{}^r$, V vs Fc/Fc^+
GC	redn	I	−1.567	75	−1.529
		II	−2.150	*b*	*b*
	oxidn	III	+0.567	103	+0.516
		IV	+0.690	90	+0.645
		V	+1.067	*b*	*b*
Au	redn	I	−1.576	75	−1.538
		II	−2.166	*b*	
	oxidn	III	+0.546	67	+0.512
		IV	+0.676	62	+0.645
		V	+1.023	*b*	*b*
Pt	redn	I	−1.579	81	−1.538
		II	−2.160	*b*	*b*
	oxidn	III	+0.535	67	+0.501
		IV	+0.683	76	+0.645
		V	+1.134	*b*	*b*
Hg	redn	I	−1.617	77	−1.579
		II	−2.199	*b*	*b*

[a] E_p = peak potential for reduction or oxidation as appropriate, ΔE_p = peak separation for oxidation and reduction process, $E_{1/2}{}^r$ = calculated reversible half-wave potential. $E_{1/2}{}^r$ for oxidation of ferrocene is 0.462 V vs Ag/AgCl. [b] Chemically irreversible process under specified conditions.

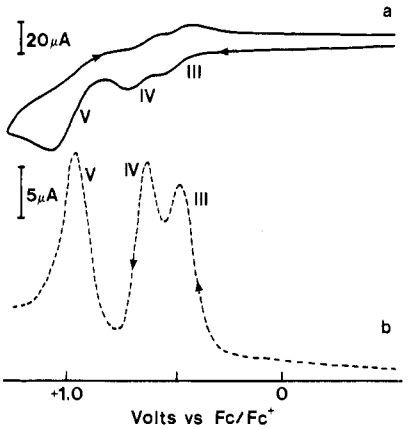

Figure 2. Cyclic (a) and differential-pulse voltammograms (b) for the oxidation of $L(S)Ni_2(pz)$ in CH_2Cl_2 (0.1 M Bu_4NClO_4) at a glassy-carbon electrode at 20 °C: (a) scan rate = 100 mV s^{-1}; (b) scan rate = 4 mV s^{-1}, pulse amplitude = 50 mV, pulse width = 60 ms, duration between pulses = 1 s.

While $[L(S)Ni_2(pz)]^+$ and $[L(S)Ni_2(pz)]^{2+}$ are written as 4-coordinate species, it is possible that the electrolyte weakly interacts with the formally nickel(III) moieties.

At more positive potentials, a multielectron oxidation process V is also observed, which is chemically irreversible at all scan rates examined (20–500 mV s^{-1}). Figure 2 also includes a small amplitude differential pulse voltammogram (Figure 2b). Under these conditions, processes III and IV are resolved as two peaks of similar height and shape. The separation in differential-pulse peak potential, which should be approximately equal to the separation in reversible half-wave potential, $(\Delta E_{1/2}{}^r)_{III,IV}{}^{ox}$, is approximately 128 ± 5 mV. This value is considerably different from $(\Delta E_{1/2}{}^r)_{I,II}{}^{red}$. Rotating disk electrode and cyclic voltammetric experiments confirm that process V is a multielectron-oxidation process at ambient temperature. At low temperatures, the onset of chemical reversibility is observed, and process V becomes split into two closely spaced one-electron-oxidation waves. Thus, formally nickel(IV) binuclear complexes appear to be generated at low temperatures on the voltammetric time scale in dichloromethane.

Data in Table I summarize a range of experimental results at Pt, Au, GC, and Hg electrodes for processes III, IV, and V in CH_2Cl_2 (0.1 M Bu_4NClO_4) at 20 °C. This and other data obtained suggest that the oxidation processes III and IV are es-

Table II. Electrochemical Data for Reduction and Oxidation of 5×10^{-4} M $L(S)Ni_2(pz)$ in Different Solvents (0.1 M Bu_4NClO_4) at a Glassy-Carbon Electrode at 20 °C[a]

			cyclic voltammetry[b]			differential pulse voltammetry[c]	
solvent	redox process		E_p, V vs Fc/Fc^+	ΔE_p, mV	$E_{1/2}^r$, V vs Fc/Fc^+	$E_{1/2}^r$, V vs Fc/Fc^+	$\Delta E_{1/2}^r$,[d] mV
CH_2Cl_2	redn	I	−1.567	75	−1.529		
			(−1.666)[e]	(65)[e]	(−1.633)[e]	(−1.633)[e]	
		II	−2.150	*f*	*f*		(556)[e]
			(−2.224)[e]	(77)[e]	(−2.185)[e]	(−2.189)[e]	
	oxidn	III	+0.567	103	+0.516	+0.519	128
		IV	+0.690	90	+0.645	+0.647	
		V	+1.067	*f*	*f*	+0.979[f]	
acetone[g]	redn	I	−1.589[h]	80[h]	−1.549[h]	−1.550	555
		II	−2.150[h]	92[h]	−2.104[h]	−2.110	
	oxidn	VI (III + IV)[i]	+0.612	*i*	*i*	+0.578	~60[i,j]
		V	+0.756	*f*	*f*	+0.701	
THF	redn	I	−1.648	103	−1.596	−1.607	524
		II	−2.167	100	−2.117	−2.131	
	oxidn	III	+0.491	*j*	*j*	+0.462	90
		IV	+0.614	*j*	*j*	+0.552	
		V	+0.807	*f*	*f*	+0.720	
DMF	redn	I	−1.559	79	−1.520	−1.520	564
		II	−2.123	91	−2.078	−2.084	
	oxidn	VI (III + IV)[i]	+0.432	*f*	*f*	+0.374	≤(40)[e,j]
		VII (V)	+0.648	*f*	*f*	+0.582	

[a] The reversible half-wave potential, $E_{1/2}^r$, for oxidation of ferrocene is +0.462 (CH_2Cl_2), +0.418 (acetone), +0.501 (THF), +0.563 (DMF), or +0.451 V vs Ag/AgCl (PrCN). [b] Scan rate = 100 mV s^{-1} unless otherwise stated. Symbols are as defined in Table I. [c] Scan rate = 4 mV s^{-1}. Conditions: pulse amplitude, 50 mV; pulse duration, 60 ms; duration between pulses, 1 s. [d] The separation in reversible half-wave potential between first and second processes for reduction or oxidation which in the text are designated as $(\Delta E_{1/2}^r)_{I,II}^{red}$ and $(\Delta E_{1/2}^r)_{I,II}^{ox}$, respectively. [e] The values in parentheses were obtained at −70 °C and a scan rate of 1 V s^{-1}. [f] Chemically irreversible process under specified conditions. [g] Saturated solution of $L(S)Ni_2(pz)$ (≤10^{-4} M). [h] Scan rate = 5 V s^{-1}. [i] Oxidation processes III and IV are not completely resolved. [j] Oxidation processes III and IV are insufficiently resolved for accurate calculations to be made.

sentially independent of electrode material (Pt, Au, GC, and Hg) and electrolyte (Et_4NClO_4, Bu_4NClO_4, Bu_4NBF_4, and Bu_4NPF_6) and vary with temperature (20 to −70 °C) as theoretically expected for a reversible electrode process whereas the nature of process V is very temperature dependent.

(c) Reduction of $L(S)Ni_2(pz)$ in Polar and Coordinating Solvents. Comparative data for reduction of $L(S)Ni_2(pz)$ in dichloromethane, DMF, acetone, THF, and PrCN at a GC electrode are collected in Table II. In the thermodynamic sense, $(E_{1/2}^r)_I^{red}$ and $(E_{1/2}^r)_{II}^{red}$ vary only slightly with the solvent and the difference $(\Delta E_{1/2}^r)_{I,II}^{red}$ is essentially independent of solvent. By contrast, kinetic differences are quite profound with respect to process II.

(i) DMF. At ambient temperature, both reduction process I and II are reversible one-electron steps in DMF (Figure 3) and occur at almost the same potential as in CH_2Cl_2, assuming that the $Fc \rightleftharpoons Fc^+ + e^-$ process is solvent independent.

The polar and potentially coordinating solvent DMF appears to substantially stabilize the reduced binuclear complexes in the kinetic sense, relative to the nonpolar noncoordinating dichloromethane solvent.

The addition of DMF to a CH_2Cl_2 solution of $L(S)Ni_2(pz)$ essentially leaves the visible spectrum (λ = 644 nm, ϵ = 3030) of $L(S)Ni_2(pz)$ unaltered (see comparison with $L(O)Ni_2(pz)$ later). It is therefore concluded that DMF does not strongly interact with $L(S)Ni_2(pz)$ and that the interaction with DMF occurs in the reduced state. Electrode process I in DMF is consistent with eq 5. That is, structural rearrangement (if any) and stabilization

$$L(S)Ni_2(pz) + e^- \rightleftharpoons [L(S)Ni_2(pz)]^- + DMF \rightleftharpoons \{[L(S)Ni_2(pz)]^- \cdots (DMF)\} \quad (5)$$

of the anion by electrostatic interaction with polar DMF would occur after electron transfer. Process II in DMF may therefore be represented as

$$\{[L(S)Ni_2(pz)]^- \cdots (DMF)\} + e^- \rightleftharpoons \{[L(S)Ni_2(pz)]^{2-} \cdots (DMF)\} \quad (6)$$

Whereas nonsolvated $[L(S)Ni_2(pz)]^{2-}$ in CH_2Cl_2 is extremely reactive and requires temperatures of −70 °C to be observed, the solvated form of the formally nickel(I) dinegative complex in DMF is considerably stabilized and can be observed on the voltammetric time scale even at room temperature. Thermodynamic stabilization of a dinegative anion attributed to nonspecific interaction has also been postulated for the reduction of copper binuclear complexes in DMF.[16]

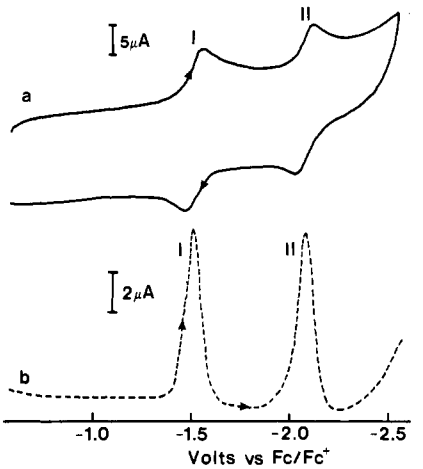

Figure 3. Cyclic (a) and differential-pulse voltammograms (b) for the reduction of $L(S)Ni_2(pz)$ in DMF (0.1 M Bu_4NClO_4) at a glassy-carbon electrode at 20 °C: (a) scan rate = 100 mV s^{-1}; (b) scan rate = 4 mV s^{-1}, pulse amplitude = −50 mV, pulse width = 60 ms, duration between pulses = 1 s.

(ii) Acetone. Acetone is expected to be a less coordinating and less polar solvent than DMF. Unfortunately, $L(S)Ni_2(pz)$ is only sparingly soluble in acetone and only limited data can be obtained. However, both reduction processes are reversible at ambient temperature (scan rate = 5 V s^{-1}) and $\{[L(S)Ni_2(pz)]^{2-} \cdots (acetone)\}$ is stabilized relative to $[L(S)Ni_2(pz)]^{2-}$ in dichloromethane.

(iii) THF. Two well-defined chemically reversible reduction processes are observed at room temperature, and the reduced species are again kinetically stabilized relative to the case in the nonpolar noncoordinating solvent dichloromethane.

(iv) General Conclusion Concerning Reduction in Polar and Coordinating Solvents. While in DMF, acetone, THF, and PrCN the reduction potentials remain essentially unchanged from the

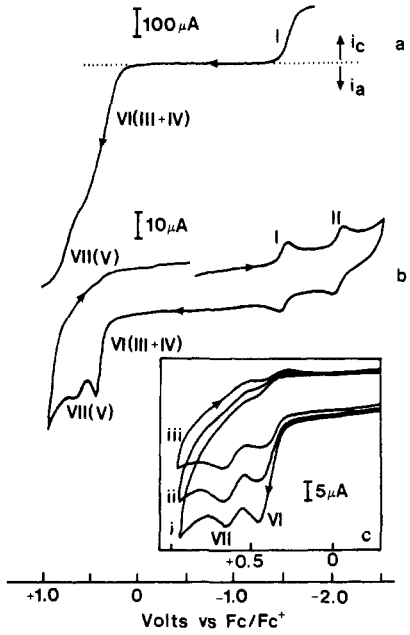

Figure 4. Rotating disk (a) and cyclic voltammograms (b, c) for L(S)-$Ni_2(pz)$ in DMF (0.1 M Bu_4NClO_4) at a glassy-carbon electrode: (a) scan rate = 20 mV s^{-1}, T = 20 °C; (b) scan rate = 100 mV s^{-1}, T = 20 °C; (c) scan rate = 100 mV s^{-1} at (i) 20, (ii) −20, and (iii) −60 °C.

value in dichloromethane, these solvents considerably stabilize the formally nickel(I), d^9, anionic, binuclear complexes in the kinetic sense. The reduction processes are consistent with the general equations

$$L(S)Ni_2(pz) + e^- \rightleftharpoons [L(S)Ni_2(pz)]^- + \text{solvent} \rightleftharpoons \{[L(S)Ni_2(pz)]^-\cdots(\text{solvent})\} \quad (7)$$

$$\{[L(S)Ni_2(pz)]^-\cdots(\text{solvent})\} + e^- \rightleftharpoons \{[L(S)Ni_2(pz)]^{2-}\cdots(\text{solvent})\} \quad (8)$$

Both the polarity and coordination ability of the solvent are important in the stabilization.

(d) Oxidation of L(S)Ni_2(pz) in Coordinating Solvents. Oxidation data at 20 °C are summarized in Table II. In contrast to the reduction data, substantial complexity is observed in the oxidation processes in coordinating solvents.

(i) DMF. In contrast to the two reversible one-electron-oxidation processes observed in CH_2Cl_2, where the species $[L(S)Ni_2(pz)]^+$ and $[L(S)Ni_2(pz)]^{2+}$ are stable on the voltammetric time scale at ambient temperatures, an unresolved overall irreversible two-electron-oxidation reduction (process VI) consisting of at least two processes (III + IV) and a further small oxidation peak at more positive potentials (process VII or process V) is observed in DMF.

Parts a and b of Figure 4 show rotating disk and cyclic voltammograms at a glassy-carbon electrode at room temperature. The limiting current per unit concentration of process VI at a rotating disk electrode is approximately twice that for the known one-electron-reduction steps. The slope of the plot of E vs log $[(i_d - i)/i]$ is 100 mV. As the temperature is lowered, process VI splits into two processes each of equal height, the ratio of process VI (III + IV) to VII approaches unity (Figure 4c), and the onset of chemical reversibility is observed. At fast scan rates and low temperatures both processes VI and VII are approximately equivalent to an overall two-electron-transfer step with process VI being split into two one-electron processes. (Diffusion coefficient changes with temperature have been allowed for via comparison with CH_2Cl_2 data.)

As data in Table II demonstrate, process VI (III + IV) occurs at a less positive potential than processes III and IV in CH_2Cl_2. At low temperature or fast scan rates the data for process VI are consistent with two unresolved one-electron processes III and IV and are similar to that in CH_2Cl_2. A mechanism that is consistent with the data at low temperatures for process VI is given in eq

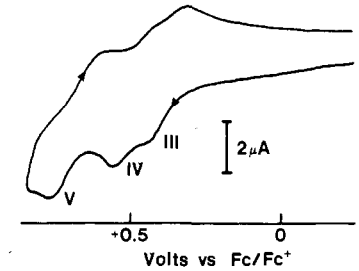

Figure 5. Cyclic voltammogram for the oxidation of L(S)Ni_2(pz) in THF (0.1 M Bu_4NClO_4) at a glassy-carbon electrode at −70 °C and a scan rate of 100 mV s^{-1}.

9. At room temperature $[L(S)Ni_2(DMF)_4]^{2+}$ and/or $[L(S)Ni_2(pz)(DMF)_2]^+$ are unstable.

$$L(S)Ni_2(pz) \rightleftharpoons [L(S)Ni_2(pz)]^+ + e^- \quad (9a)$$

$$[L(S)Ni_2(pz)]^+ + 2DMF \rightleftharpoons [L(S)Ni_2(pz)(DMF)_2]^+ \quad (9b)$$

$$[L(S)Ni_2(pz)(DMF)_2]^+ \rightleftharpoons [L(S)Ni_2(pz)(DMF)_2]^{2+} + e^- \quad (9c)$$

$$[L(S)Ni_2(pz)(DMF)_2]^{2+} + 2DMF \rightleftharpoons [L(S)Ni_2(pz)(DMF)_4]^{2+} \quad (9d)$$

At low temperature and fast scan rates the reaction parallels that in CH_2Cl_2 with a temperature-dependent solvent term being present. However, unlike the reduction processes, solvent effects cannot be attributed to nonspecific solvent terms. Rather solvent coordination to produce an increased coordination number around nickel must be invoked. Nickel(III) complexes are usually 6-coordinate.[7b,7c,24] Oxidation of monomeric nickel(II) complexes is known to involve participation of the solvent and/or electrolyte.[25] The chemical irreversibility in DMF at ambient temperatures may be attributed to structural rearrangement after electron transfer as in eq 10 where the nonspecifically designated ligands surrounding Ni^{III} are assumed to be DMF (or perchlorate).

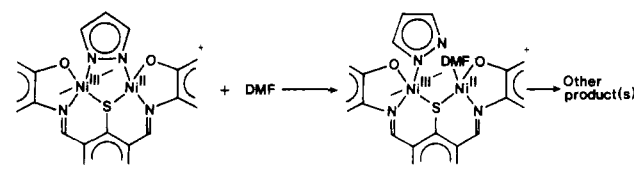

(10)

(ii) Acetone and THF. In acetone, two chemically irreversible oxidation processes VI (III + IV) and VII (V) are observed for cyclic voltammetry. The differential-pulse voltammogram also shows one major oxidation process followed by a minor process. Unfortunately, solubility problems prevented examination at low temperatures. However, results can be assumed to be similar to those in DMF.

In THF, cyclic voltammetry exhibits three oxidation processes, in which the first two oxidation steps but not the third are reversible at room temperature. The potential separation and behavior of the first two oxidation processes are similar to those observed in CH_2Cl_2. Reactions III and IV in THF can be described by the overall equations (11) and (12). The potential

$$L(S)Ni_2(pz) + 2THF \rightleftharpoons [L(S)Ni_2(pz)(THF)_2]^+ + e^- \quad (11)$$

$$[L(S)Ni_2(pz)(THF)]^+ + 2THF \rightleftharpoons [L(S)Ni_2(pz)(THF)_4]^{2+} + e^- \quad (12)$$

difference $(\Delta E_{1/2}^r)_{III,IV}^{ox}$ between the first two oxidation processes

(24) (a) Lovecchio, F. V.; Gore, E. S.; Busch, D. H. *J. Am. Chem. Soc.* **1974**, *96*, 3109. (b) Bossu, F. P.; Margerum, D. W. *Inorg. Chem.* **1977**, *16*, 1210. (c) Fabbrizzi, L. *Comments Inorg. Chem.* **1985**, *4*, 33.

(25) (a) Zeigerson, E.; Bar, I.; Bernstein, J.; Kirschenbaum, L. J.; Meyerstein, D. *Inorg. Chem.* **1982**, *21*, 73. (b) Buttafava, A.; Fabrizzi, L.; Perotti, A.; Poggi, A.; Poli, G.; Seghi, B. *Inorg. Chem.* **1986**, *25*, 1456. (c) Fabbrizzi, L.; Licchelli, M.; Perotti, A.; Poggi, A.; Soresi, S. *Isr. J. Chem.* **1985**, *25*, 112. (d) Kimura, E.; Machida, R.; Kodama, M. *J. Am. Chem. Soc.* **1984**, *106*, 5497. (e) Sabatini, L.; Fabbrizzi, L. *Inorg. Chem.* **1979**, *18*, 438.

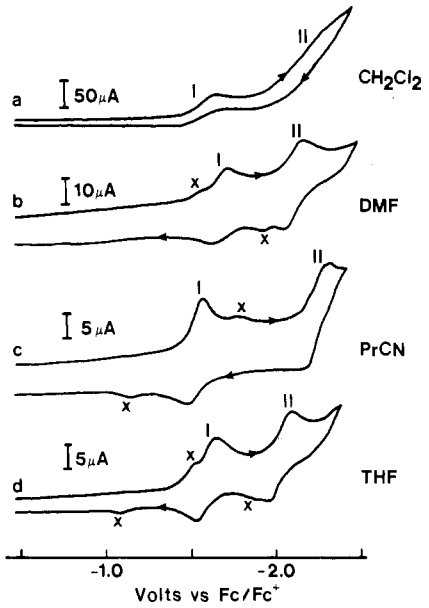

Figure 6. Cyclic voltammograms for the reduction of $L(O)Ni_2(pz)$ in (a) CH_2Cl_2, (b) DMF, (c) PrCN, and (d) THF (0.1 M Bu_4NClO_4) at a glassy-carbon electrode at 20 °C and a scan rate of 100 mV s^{-1}.

is approximately 90 mV, which is slightly less than that in CH_2Cl_2 (135 mV). These potential differences enable the comproportionation constant for reaction 13 to be calculated. The value is

$$Ni^{II}{}_2 + [Ni^{III}{}_2]^{2+} \overset{K}{\rightleftharpoons} 2[Ni^{II}Ni^{III}]^{+} \qquad (13)$$

a measure of the strength of interaction in binuclear complexes after a one-electron transfer.[25,26] Thus, $(\Delta E_{1/2}{}^{r})_{III,IV}{}^{ox}$ values suggest that the presence of coordinating solvents results in a weakening of the binuclear interactions in the oxidized mixed-valence complex. In THF at low temperatures, process V approaches a chemically reversible two-electron oxidation (Figure 5) to produce a formally nickel(IV) complex, $[L(S)Ni_2(pz)(THF)_x]^{4+}$. Nickel(IV) complexes are almost invariably 6-coordinate so that x can be presumed to be 4.[7b] That is, the electron-transfer processes

$$[L(S)Ni_2(pz)(solvent)_4]^{2+} \rightleftharpoons [L(S)Ni_2(pz)(solvent)_4]^{3+} + e^- \qquad (14)$$

$$[L(S)Ni_2(pz)(solvent)_4]^{3+} \rightleftharpoons [L(S)Ni_2(pz)(solvent)_4]^{4+} + e^- \qquad (15)$$

occur at very similar potentials. However, the products are highly reactive.

(e) Controlled-Potential Electrolysis of $L(S)Ni_2(pz)$. Controlled-potential reductive electrolysis of $L(S)Ni_2(pz)$ in CH_2Cl_2, DMF, or THF at −1.75 V vs Fc/Fc^+ (between process I and II) or at a more negative potential than process II confirms the instability of $[L(S)Ni_2(pz)]^-$ and $[L(S)Ni_2(pz)]^{2-}$ predicted from voltammetric time scale measurements in CH_2Cl_2 where no nonspecific stabilization is present. Coulometric data are consistent with multielectron reduction processes on the long time scale and complete decomposition of the reduced binuclear species.

Controlled-potential oxidative electrolysis in THF at +0.650 V vs Fc/Fc^+ consumed approximately 2 mol of electrons/mol of complex at 0 °C. The cyclic voltammetry after electrolysis gave three new reversible waves with $E_{1/2}{}^{r}$ values of −0.035, −0.950, and −1.976 V vs Fc/Fc^+. The $E_{1/2}$ values do not correspond to formation of $[L(S)Ni_2(pz)]^{2+}$. The new oxidized product(s) has not been characterized. Similarly, no evidence for formation of $[L(S)Ni_2(pz)]^{2+}$ could be found after controlled-potential oxidative electrolysis in CH_2Cl_2 or DMF.

$L(O)Ni_2(pz)$. (a) Reduction of $L(O)Ni_2(pz)$ in CH_2Cl_2. The complex $L(O)Ni_2(pz)$ in CH_2Cl_2 exhibits two reduction processes that are shown in Figure 6a and are again labeled processes I and II for comparison purposes with the sulfur analogue. However, unlike the case with $L(O)Ni_2(pz)$, no reverse peak is observed on the reverse (oxidative) potential scan direction even at low temperature and fast scan rates when the potential is switched after process I. The limiting current per unit concentration at a dropping mercury electrode or rotating disk electrode corresponds to a multielectron reduction process.

The second reduction process, process II, is drawn out and not well-defined, although a multielectron process must be involved based on the current magnitudes observed in cyclic and rotating disk voltammograms.

The data suggest that the reduced species $[L(O)Ni_2(pz)]^-$ is not stable even on the voltammetric time scale in CH_2Cl_2. Table III shows that reduction processes I and II for $L(O)Ni_2(pz)$ are almost independent of the electrode material (Au, GC, Pt, and Hg).

(b) Oxidation of $L(O)Ni_2(pz)$ in CH_2Cl_2. The cyclic voltammograms of $L(O)Ni_2(pz)$ in CH_2Cl_2 (Figure 7a) show two well-defined processes (VIII and IX). Response VIII is chemically

Table III. Cyclic Voltammetric Data for Reduction and Oxidation of $L(O)Ni_2(pz)$ in CH_2Cl_2 (0.1 M Bu_4NClO_4) at 20 °C Using a Scan Rate of 100 mV s^{-1} [a]

electrode	process		E_p, V vs Fc/Fc^+	ΔE_p, mV	$E_{1/2}$, V vs $Fc^{0/+}$
GC	redn	I	−1.638	[b]	[b]
		II	−2.239	[b]	[b]
	oxidn	VIII (III + IV)	+0.485[c]	125[c]	+0.422[c]
		IX (V)	+0.874	[b]	[b]
Au	redn	I	−1.643	[b]	[b]
		II	−2.259	[b]	[b]
	oxidn	VIII (III + IV)	+0.492[c]	121[c]	+0.432[c]
		IX (V)	+0.892		
Pt	redn	I	−1.70	[b]	[b]
		II	−2.30	[b]	[b]
	oxidn	VIII (III + IV)	+0.485[c]	133[c]	+0.419[c]
		IX (V)	+0.830	[b]	[b]
Hg	redn	I	−1.659	[b]	[b]
		II	−2.225	[b]	[b]

[a] Symbols are the same as used in Table I except that $E_{1/2}$ is not a reversible half-wave potential. Rather, it is data calculated from an unresolved two-electron-oxidation process. [b] Chemically irreversible process under specified conditions. [c] Unresolved overall two-electron-oxidation process.

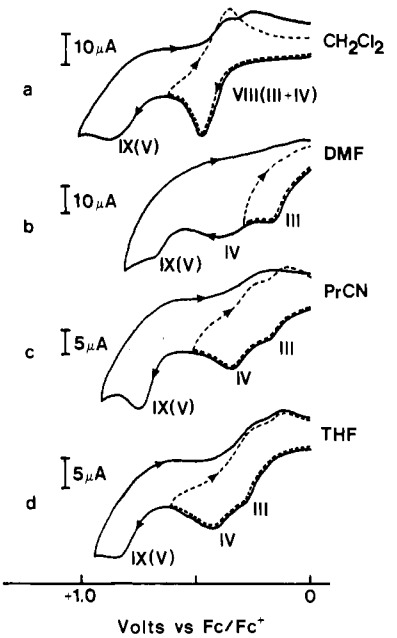

Figure 7. Cyclic voltammograms for the oxidation of $L(O)Ni_2(pz)$ in (a) CH_2Cl_2, (b) DMF, (c) PrCN, and (d) THF (0.1 M Bu_4NClO_4) at a glassy-carbon electrode at 20 °C and a scan rate of 100 mV s^{-1}.

(26) Creutz, C. *Prog. Inorg. Chem.* **1983**, *30*, 1.

Table IV. Electrochemical Data for Reduction and Oxidation of 5×10^{-4} M $L(O)Ni_2(pz)$ in Different Solvents (0.1 M Bu_4NClO_4) at a Glassy-Carbon Electrode at 20 °C

			cyclic voltammetry[a]			differential-pulse voltammetry[a]	
solvent	redox process		E_p, V vs Fc/Fc^+	ΔE_p, mV	($E_{1/2}^r$ or $E_{1/2}$), V vs Fc/Fc^+	($E_{1/2}^r$ or $E_{1/2}$), V vs Fc/Fc^+	($\Delta E_{1/2}^r$ or $\Delta E_{1/2}$), mV
CH_2Cl_2	redn	I	−1.638	*b*	*b*	*b*, *c*	~600
		II	−2.239	*b*	*b*	*b*, *c*	
	oxidn	VIII (III + IV)	+0.485	125	+0.422	+0.438	≤40
		IX (V)	+0.874	*b*	*b*	*b*	
acetone[d,e]	redn	I	(−1.672)[f]	(147)[f]	(−1.599)[f]	*b*, *c*	(~500)[f]
		II	(−2.182)[f]	(129)[f]	(−2.118)[f]	*b*, *c*	
	oxidn	III	+0.297	86	+0.254	+0.243	~150
		IV	+0.448	76	+0.410	+0.395	
		V	+0.748	*b*	*b*	*b*, *c*	
THF[d,e]	redn	I	−1.701	109	−1.647	−1.638	~450
		II	−2.139	121	−2.079	−2.086	
	oxidn	III	+0.303	147	+0.230	+0.232	~130
		IV	+0.432	148	+0.358	+0.356	
		V	+0.854	*b*	*b*	+0.768[b]	
PrCN[d,e]	redn	I	−1.543	86	−1.500	−1.508	~700
		II	−2.248	*b*	*b*	−2.184	
	oxidn	III	+0.200	64	+0.168	+0.166	~150
		IV	+0.350	117	+0.308	+0.298	
		V	+0.768	*b*	*b*	+0.722	
DMF[d,e]	redn	I	−1.740	104	−1.688	−1.688	~400
		II	−2.112	72	−2.07	−2.096	
	oxidn	III	+0.181	*b*	*b*	*b*	~200
		IV	+0.380	*b*	*b*	*b*	
		VIII (V)	+0.706	*b*	*b*	+0.662[b]	
		(III + IV)[f]	(+0.141)[f]	(89)[f]	(+0.086)[f]	(+0.064)[f]	≤40
		IX (V)[f]	(+0.802)[f]	*b*	*b*	(+0.652)[b,f]	

[a] Scan rate = 100 mV s^{-1} for cyclic voltammetry and 4 mV s^{-1} for differential-pulse voltammetry. Symbols and parameters are as defined in Tables I–III. [b] Chemically irreversible process under specified conditions. [c] Broad and ill-defined. [d] Minor peaks for reduction and oxidation processes are observed in this solvent under conditions of cyclic voltammetry. See text and figures. [e] The reduction and oxidation waves show substantial temperature and scan rate dependence: see text and figures. [f] Data obtained at −60 °C.

reversible when the potential is reversed at +0.6 V vs Fc/Fc^+. The limiting current per unit concentration in rotating disk voltammetry for process VIII corresponds to a two-electron process. Data indicate that this electrode reaction is an overall chemically reversible two-electron-oxidation process

$$[L(O)Ni_2(pz)] \rightleftharpoons [L(O)Ni_2(pz)]^{2+} + 2e^- \quad (16)$$

By contrast, $L(S)Ni_2(pz)$ gives two closely spaced reversible one-electron steps that apparently are unresolved with $L(O)Ni_2(pz)$. Process VIII is therefore equivalent to the summation of processes III and IV and is designated this way in the tables and figures. Process VIII is sensitive to impurities such as H_2O, which lead to a loss of chemical reversibility.

Process IX is chemically irreversible at all scan rates and temperatures examined. Process IX presumably involves a reaction of the kind

$$[L(O)Ni_2(pz)]^{2+} \rightleftharpoons [L(O)Ni_2(pz)]^{4+} + 2e^- \quad (17)$$

which is analogous to process V for the $L(S)Ni_2(pz)$ case.

(c) Reduction of $L(O)Ni_2(pz)$ in Polar and Coordinating Solvents. Electrochemical data for reduction of $L(O)Ni_2(pz)$ in CH_2Cl_2, DMF, THF, acetone, and PrCN are collected in Table IV. In contrast to the almost solvent-independent behavior of $L(S)Ni_2(pz)$, reduction data for $L(O)Ni_2(pz)$ are extremely solvent dependent.

(i) DMF. Cyclic voltammograms (Figure 6b) exhibit two well-defined reduction waves I and II, both of which are chemically reversible at room temperature. This result should be contrasted with data in dichloromethane where no reversible reduction processes are observed for reduction of $L(O)Ni_2(pz)$. Furthermore, the separation of $(\Delta E_{1/2}^r)_{I,II}^{red}$ is 160 mV less than $(\Delta E_{1/2}^r)_{I,II}^{red}$ for $L(S)Ni_2(pz)$ in DMF. Additional peaks, which are labeled with a cross (×) in Figure 6b are also present. When the temperature is lowered, the first reduction process becomes broad and complex. However, the second process and the reverse peak of process I remain sharp and only alter marginally with temperature (Figure 8). This temperature dependence of the voltammograms is totally reproducible on either increasing or decreasing the temperature. The temperature dependence is again in marked contrast to reduction processes for $L(S)Ni_2(pz)$.

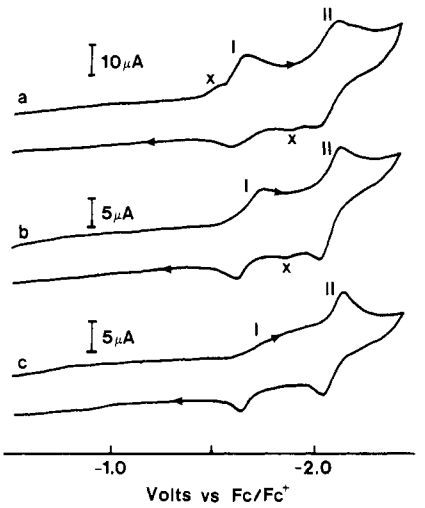

Figure 8. Temperature dependence of cyclic voltammograms for reduction of $L(O)Ni_2(pz)DMF$ (0.1 M Bu_4NClO_4) at a glassy-carbon electrode at a scan rate of 100 mV s^{-1}: (a) 25 °C; (b) −13 °C; (c) −58 °C.

Data suggest that the solution chemistry of $L(O)Ni_2(pz)$ in DMF is far more complex than that for $L(S)Ni_2(pz)$. $L(O)Ni_2(pz)$ could be recrystallized from dimethylformamide solution as a mono-DMF solvate, which showed an effective magnetic moment at room temperature of 1.64 μ_B per nickel. This result is suggestive of one diamagnetic, square-planar nickel center and one paramagnetic nickel center per molecule, with dimethylformamide occupying the fifth donor site in the latter case. This dimethylformamide ligand is evidently weakly bound because when the solvated material was recrystallized from chloroform, the crystalline nonsolvated solid separated. The ^1H NMR spectrum of the mono-DMF solvate in deuteriochloroform was merely a

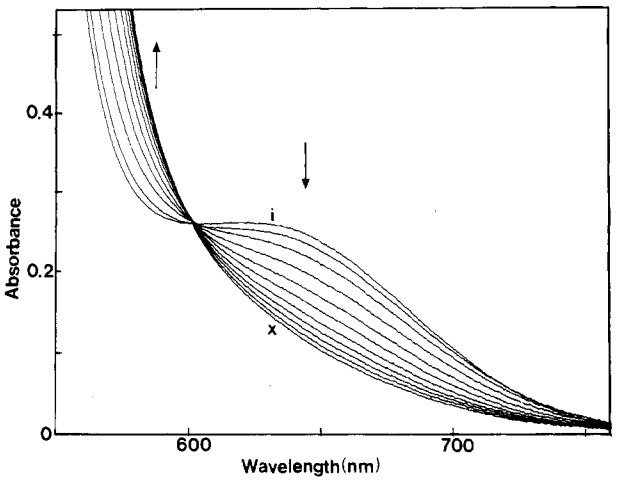

Figure 9. Absorption spectra of 5.4×10^{-4} M $L(O)Ni_2(pz)$ in CH_2Cl_2 at 20 °C with varying concentrations of DMF. [DMF] = (i) 0.416, (ii) 0.833, (iii) 1.250, (iv) 1.666, (v) 2.083, (vi) 2.499, (vii) 2.916, (viii) 3.332, (ix) 3.749, and (x) 4.160 M.

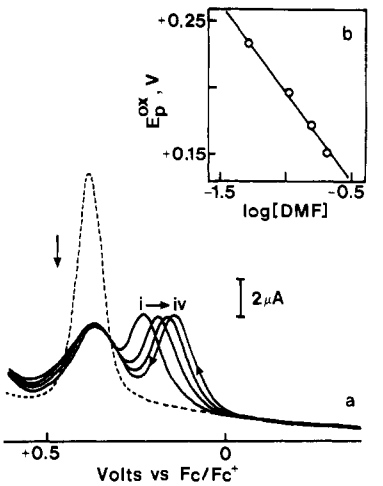

Figure 10. (a) Differential-pulse voltammograms for oxidation of 5.4×10^{-4} M $L(O)Ni_2(pz)$ in CH_2Cl_2 at a glassy-carbon electrode at 20 °C in the absence (---) and in the presence (—) of different concentrations of DMF. [DMF] = (i) 0.049, (ii) 0.102, (iii) 0.153, and (iv) 0.204, M. Scan rate = 4 mV s^{-1}, pulse amplitude = 50 mV, pulse width = 60 ms, and duration between pulses = 1 s. (b) Plot of peak potential for oxidation vs log [DMF].

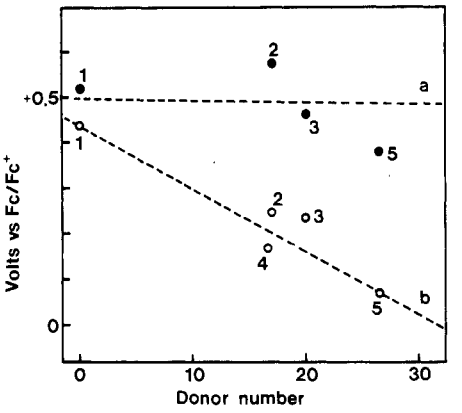

Figure 11. Plot of the first oxidation potential, $(E_{1/2}^{r}$ or $E_{1/2})_{III}$ at 20 °C vs Gutmann's donor number in different solvents for (a) $L(S)Ni_2(pz)$ and (b) $L(O)Ni_2(pz)$: (1) CH_2Cl_2; (2) acetone; (3) THF; (4) PrCN; (5) DMF.

superimposition of the individual spectra of $L(O)Ni_2(pz)$ and dimethylformamide in 1:1 proportions, which is consistent with complete dissociation of dimethylformamide from the nickel, leaving it diamagnetic under these conditions. However, in neat dimethylformamide solution both nickel centers become paramagnetic, the effective moment per nickel being 3.3 μ_B, suggesting that both nickel centers had taken on at least one dimethylformamide. The only discernible features attributable to L(O) in the ^1H NMR spectrum of $L(O)Ni_2(pz)$ in deuteriodimethylformamide were two broad *tert*-butyl signals at approximately 2 ppm. This behavior is in sharp contrast to that of $L(S)Ni_2(pz)$, which showed essentially the same ^1H NMR features in deuteriodimethylformamide as in deuteriochloroform. Clearly, negligible binding of dimethylformamide to nickel occurs with the L(S) complex. The UV–visible electronic spectrum of $L(O)Ni_2(pz)$ in dichloromethane showed a band at 628 nm (ϵ = 520) consistent with square-planar nickel(II).[27] The effect of stepwise addition of dimethylformamide to such a dichloromethane solution is shown in Figure 9. The 628-nm band gradually disappears, and a clean isobestic point at 610 nm is observed. Analysis of the spectral changes occurring (Figure 9) in the dimethylformamide concentration range 0.4–4 M indicates the uptake of 2 molar equiv of dimethylformamide per binuclear unit with an equilibrium constant of 0.07 M^{-2} for the equilibrium

$$L(O)Ni_2(pz) + 2DMF \overset{K}{\rightleftharpoons} L(O)Ni_2(pz)(DMF)_2 \quad (18)$$

In accordance with the above data, the complex temperature dependence of cyclic voltammograms can be attributed to temperature-dependent equilibrium constants. The solvated complexes with different numbers of coordinated DMF will be reduced at similar reduction potentials, resulting in overlapping of reduction process and therefore drawn-out waves, unless all processes accompanying electron transfer are very fast. Apparently this is not the case with respect to the voltammetric time scale.

Thus, an example of electron-transfer reactions combined with the solvent coordination equilibria is as shown in eq 19. On reduction, a decrease in the overall average coordination number may occur, explaining the relative invariance of process II and reverse peak of process I with temperature. Equation 19 is necessarily a simplified version of the reduction process. Without any knowledge of the solution chemistry of $[L(O)Ni_2(pz)(solvent)_n]^-$ and $[L(O)Ni_2(pz)(solvent)_n]^{2-}$ (n = 0, 1, 2) the problem of providing a quantitative description of the reduction processes is intractable. The presence of processes additional to the main reduction steps have been noted for related binuclear complexes[7a,7e] in DMF and other coordinating solvents. The present investigation indicates that they arise from formation of solvated species.

(ii) Other Coordinating Solvents. Cyclic voltammograms of $L(O)Ni_2(pz)$ in PrCN and THF give results parallel to those obtained in DMF. In PrCN, two major one-electron-reduction peaks are observed (Figure 6c). The minor reduction peak marked with a cross (×) in Figure 6c may arise from the reduction of a solvated species present in the bulk solution or generated at the electrode surface. Labeled minor oxidation processes can be attributed to oxidation of a solvated reduction product. The first major reduction process is a one-electron process, with a considerable degree of chemical and electrochemical reversibility. No chemical reversibility is observed for the second major reduction process, process II, in PrCN at a scan rate of 200 mV s^{-1}. In contrast, at a scan rate of 2 V s^{-1} process II shows partial chemical reversibility (ΔE_p = 93 mV; i_p^{red}/i_p^{ox} = 1.44), but at the same time the first reduction wave becomes a drawn-out composite process involving overlapping responses as is the case at low temperature.

In THF (Figure 6d), two major one-electron chemically reversible processes and an additional minor wave are observed.

$L(O)Ni_2(pz)$ in acetone shows two irreversible reduction steps at scan rate 100 mV s^{-1} and room temperature. However, the processes are transformed into two chemically reversible one-electron-reduction steps at scan rates greater than 8 V s^{-1}, sug-

(27) Lever, A. B. P. *Inorganic Electronic Spectroscopy*, 2nd. ed.; Elsevier: New York, 1984; p 534.
(28) Holm, R. H.; O'Connor, M. J. *Prog. Inorg. Chem.* **1971**, *14*, 241.

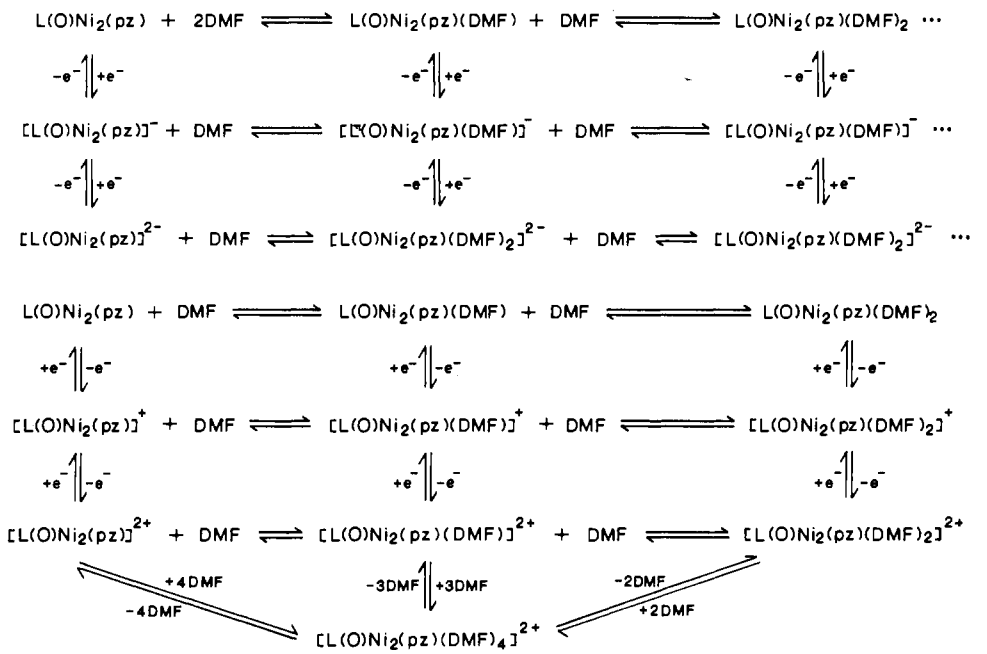

(19) (20)

gesting the reduced species $[L(O)Ni_2(pz)]^-$ and $[L(O)Ni_2(pz)]^{2-}$ are stabilized in acetone, relative to the case in CH_2Cl_2.

Solvent interactions stabilize $[L(S)Ni_2(pz)]^-$ and $[L(S)Ni_2(pz)]^{2-}$ complexes as shown previously. Similarly, solvent interactions stabilize $[L(O)Ni_2(pz)]^-$ and $L(O)Ni_2(pz)]^{2-}$. However, the reductive redox chemistry is substantially more complex in the case of $L(O)Ni_2(pz)$ reduction because of the co-existence of a range of $L(O)Ni_2(pz)(solvent)_n$ (n = 0, 1, 2, ...) complexes.

(d) Oxidation of $L(O)Ni_2(pz)$ in Coordinating Solvents. The oxidation of $L(S)Ni_2(pz)$ has been shown to involve solvation of products. With $L(O)Ni_2(pz)$, solutions of the reactant already involve a range of equilibria. Not surprisingly, oxidation of $L(O)Ni_2(pz)$, like the reduction, is therefore extremely complex.

(i) DMF. A cyclic voltammogram in Figure 7b exhibits three oxidation waves in pure DMF at a glassy-carbon electrode and room temperature (scan rate 100 mV s^{-1}). Even when the potential is reversed at +0.25 V vs Fc/Fc^+, the first (least positive) process exhibits no chemical reversibility. At −72 °C or a fast scan rate (5 V s^{-1}), only a chemically reversible two-electron wave, VIII (III + IV), and an irreversible two-electron wave, IX, are observed as is the case in dichloromethane. This is consistent with the enhanced stability of $[L(O)Ni_2(pz)]^{2+}$ at lower temperatures and temperature-dependent equilibrium and/or rate constants as noted in the reduction section.

The addition of DMF to a solution of $L(O)Ni_2(pz)$ in CH_2Cl_2 under conditions similar to the previously described spectrophotometric measurements where $L(O)Ni_2(pz)(DMF)_2$ is formed, but monitored by differential pulse voltammetry, shows a decrease in the peak height for the unresolved $[L(O)Ni_2(pz)]^{0/2+}$ oxidation process and the simultaneous appearance of a new peak (Figure 10). This new process shifts to more negative potentials as the DMF concentration increases. A slope for the plot of the differential-pulse oxidation potential E_p^{ox} vs log [DMF] is 130 mV, which is consistent with a one-electron reaction involving addition of two molecules of DMF in the first one-electron transfer. Oxidation process VIII (III + IV) at low temperatures, where products are stable, can therefore be written as shown in eq 20. This is undoubtedly a simplified form of the oxidation process, in the same sense that eq 19 is a simplified version of the reduction scheme.

(ii) PrCN and Acetone. The electrochemical data in PrCN and acetone are collected in Table III. Three oxidation processes are observed in these solvents. In PrCN (Figure 7c), the first two oxidation steps are chemically reversible when the potential is switched at +0.5 V vs Fc/Fc^+. The limiting current per unit concentration of both processes are approximately the same as reduction process I, which is a one-electron-reduction process. A negative potential shift in PrCN relative to that in CH_2Cl_2 is observed. It appears that PrCN is also coordinated to $L(O)Ni_2(pz)$ as is DMF. The electrochemical oxidation in acetone is similar to that in PrCN. The differential-pulse voltammogram of $L(O)Ni_2(pz)$ in acetone gave two well-defined one-electron-oxidation peaks, followed by an irreversible two-electron process at more positive potentials.

(iii) THF. Two close-spaced chemically reversible oxidation processes, III and IV, followed by an irreversible two electron process, V, are observed at room temperature and a scan rate of 100 mV s^{-1} (Figure 7d). The first two processes are well resolved by using differential-pulse voltammetry. The total current height of the first two oxidation processes is twice that of the first reduction process. The oxidation potential of the resolved waves in THF is approximately 200 mV more negative than that in CH_2Cl_2, which suggests that the solvent coordination occurs as in the case in DMF.

Thus, the first two oxidation processes proceed stepwise as follows:

$$L(O)Ni_2(pz)(THF)_x \rightleftharpoons [L(O)Ni_2(pz)(THF)_y]^+ + e^- \quad (21)$$

$$[L(O)Ni_2(pz)(THF)_y]^+ \rightleftharpoons [L(O)Ni_2(pz)(THF)_z]^{2+} + e^- \quad (22)$$

$$x, y, z = 0, 1, 2, 3, 4$$

Processes III and IV coalesce at −48 °C and cannot be resolved even via differential-pulse voltammetry with a small amplitude. At low temperature in THF, the response resembles the unresolved two-electron oxidation observed in CH_2Cl_2 (room temperature) and DMF (at low temperature).

Equations 23–25 summarize the electrochemical oxidation in coordinating solvents.

$$L(O)Ni_2(pz)(solvent)_x \rightleftharpoons [L(O)Ni_2(pz)(solvent)_y]^+ + e^- \quad (23)$$

$$[L(O)Ni_2(pz)(solvent)_y]^+ \rightleftharpoons [L(O)Ni_2(pz)(solvent)_z]^{2+} + e^- \quad (24)$$

$$[L(O)Ni_2(pz)(solvent)_z]^{2+} \rightleftharpoons [L(O)Ni_2(pz)(solvent)_z]^{4+} + 2e^- \quad (25)$$

$$x, y, z = 0, 1, 2, 3, 4$$

The first oxidation process for $L(O)Ni_2(pz)$ is strongly dependent on the solvent. In contrast, the potential for the first oxidation process for $L(S)Ni_2(pz)$ is relatively insensitive to the solvent. A plot of the first oxidation potential, $(E_{1/2})_{III}^{ox}$ vs Gutmann's donor number[29] is shown in Figure 11. An excellent

(29) (a) Gutmann, V. *The Donor-Acceptor Approach to Molecular Interactions*; Plenum: New York, 1978; p 20. (b) Gagné, R. R.; Ingle, D. M. *Inorg. Chem.* **1981**, *20*, 420.

correlation is observed for the $L(O)Ni_2(pz)$ complex; i.e., this complex is more easily oxidized in stronger donor solvents whereas the ease of oxidation of $L(S)Ni_2(pz)$ is almost independent of the donor number.

(e) Controlled-Potential Electrolysis of $L(O)Ni_2(pz)$. As in the case of $L(S)Ni_2(pz)$ no evidence for stable $[L(O)Ni_2(pz)]^{2+}$, $[L(O)Ni_2(pz)]^{+}$, $[L(O)Ni_2(pz)]^{-}$, or $[L(O)Ni_2(pz)]^{2-}$ species could be obtained on the time scale of controlled-potential electrolysis. This is also consistent with other studies on related binuclear nickel complexes.[7a,c]

(f) Conclusions. The electrochemistry of $L(S)Ni_2(pz)$ and $L(O)Ni_2(pz)$ is characterized by two reduction processes

$$L(X)Ni_2(pz) + e^- \rightleftharpoons [L(X)Ni_2(pz)]^- \quad \text{(process I)} \quad (26)$$

$$[L(X)Ni_2(pz)]^- + e^- \rightleftharpoons [L(X)Ni_2(pz)]^{2-} \quad \text{(process II)} \quad (27)$$

which are separated by several hundred millivolts (X = S or O). This implies that strong interaction[30] is present for the mixed-valence species $[L(X)Ni_2(pz)]^-$. $L(S)Ni_2(pz)$ is not strongly solvated, and the separation in $(\Delta E_{1/2})_{I,II}^{red}$ is essentially solvent independent. In contrast, $L(O)Ni_2(pz)$ exists as a mixture of solvated species in coordinating solvents, which influences the redox chemistry. The reduced species $[L(X)Ni_2(pz)]^-$ and $[L(X)Ni_2(pz)]^{2-}$ are stabilized by nonspecific solvent effects present in polar solvents.

Oxidation of $L(X)Ni_2(pz)$ occurs via two barely resolved one-electron oxidation processes that are extremely solvent dependent:

$$L(X)Ni_2(pz) \rightleftharpoons [L(X)Ni_2(pz)]^+ + e^- \quad \text{(process III)} \quad (28)$$

$$[L(X)Ni_2(pz)]^+ \rightleftharpoons [L(X)Ni_2(pz)]^{2+} + e^- \quad \text{(process IV)} \quad (29)$$

That is, interactions in the mixed-valent complex $[L(X)Ni_2(pz)]^+$ are very weak[30] compared to the very strong interactions associated with the anionic binuclear complex $[L(X)Ni_2(pz)]^-$. A further two-electron process produces a highly reactive formally nickel(IV) species that is stabilized in coordinating solvents such as THF.

The remarkably different solvent effects associated with $L(S)Ni_2(pz)$ and $L(O)Ni_2(pz)$ are quite surprising because the distinction between the two complexes is only an endogenous bridging atom, O vs S. Interestingly, the sulfur binuclear complex is harder to oxidize than the oxygen one, contrary to normal expectations.[31] This implies that a structural difference influences the redox data in a manner that is not presently understood but illustrates the importance of the endogenous bridging center.

Acknowledgment. Work described in this paper was financially supported by the Australian Research Grants Scheme. The award of a Deakin University Gordon Research Fellowship and the assistance of the Japanese Ministry of Education enabling M.H. to spend a year's leave in Australia are also gratefully acknowledged.

Registry No. $L(S)Ni_2(pz)$, 111005-98-2; $[L(S)Ni_2(pz)]^-$, 111006-00-9; $[L(S)Ni_2(pz)]^{2-}$, 111006-01-0; $[L(S)Ni_2(pz)]^+$, 111006-02-1; $[L(S)Ni_2(pz)]^{2+}$, 111006-03-2; $L(O)Ni_2(pz)$, 111005-99-3; $[L(O)Ni_2(pz)]^-$, 111006-04-3; $[L(O)Ni_2(pz)]^{2-}$, 111006-05-4; $[L(O)Ni_2(pz)]^+$, 111006-06-5; $[L(O)Ni_2(pz)]^{2+}$, 111006-07-6; $L(O)Ni_2(pz)(DMF)_2$, 111006-08-7; DMF, 68-12-2; THF, 109-99-9; $L(S)H_2(C(O)NMe_2)$, 110480-99-4; $L(O)H_3$, 111006-09-8; C, 7440-44-0; Au, 7440-57-5; Pt, 7440-06-4; Hg, 7439-97-6; CH_2Cl_2, 75-09-2; PrCN, 109-74-0; acetone, 67-64-1; 2-amino-4,6-di-*tert*-butylphenol, 1643-39-6; 2-((*N*,*N*-dimethylcarbamoyl)thio)-5-methylisophthalaldehyde, 73729-07-4; 2-hydroxy-5-methylisophthalaldehyde, 7310-95-4.

(30) Robin, M. B.; Day, P. *Adv. Inorg. Chem. Radiochem.* **1967**, *10*, 247.

(31) Ray, D.; Pal, S.; Chakravorty, A. *Inorg. Chem.* **1986**, *25*, 2674.

Contribution from the Lehrstuhl für Anorganische Chemie I der Ruhr-Universität, D-4630 Bochum, FRG, Department of Chemistry and Laboratory for Molecular Structure and Bonding, Texas A&M University, College Station, Texas 77843, and Anorganisch-Chemisches Institut der Universität, D-6900 Heidelberg, FRG

Syntheses and Spectroscopic and Magnetic Properties of Novel Binuclear Vanadium(III/IV) Complexes. Crystal Structures of $[L_2V_2(\mu\text{-}O)(\mu\text{-}CH_3CO_2)_2]I_2\cdot 2H_2O$ and $[L_2V_2O_2(\mu\text{-}CH_3CO_2)_2]I_2$ (L = 1,4,7-Trimethyl-1,4,7-triazacyclononane)

Martin Köppen,[1a] Gerd Fresen,[1a] Karl Wieghardt,*[1a] Rosa M. Llusar,[1b] Bernhard Nuber,[1c] and Johannes Weiss[1c]

Received August 6, 1987

Hydrolysis of $[LVCl_3]\cdot$dmf (dmf = dimethylformamide) in aqueous sodium acetate solution under anaerobic conditions yields the green binuclear dication $[L_2V_2(\mu\text{-}O)(\mu\text{-}CH_3CO_2)_2]^{2+}$, which has been isolated as the diiodide dihydrate (L = 1,4,7-trimethyl-1,4,7-triazacyclononane, $C_9H_{21}N_3$). $[L_2V_2(\mu\text{-}O)(\mu\text{-}CH_3CO_2)_2]I_2\cdot 2H_2O$ crystallizes in the monoclinic system, space group $P2_1/c$, with $a = 8.836$ (5) Å, $b = 21.637$ (6) Å, $c = 18.560$ (7) Å, $\beta = 103.09$ (5)°, and $Z = 4$. The two vanadium(III) centers (d^2–d^2) are ferromagnetically spin exchange coupled ($H = -2J\hat{S}_1\hat{S}_2$; $S_1 = S_2 = 1$; $J = +22$ cm^{-1}; $g = 2.1$). Air oxidation of this green complex affords blue crystals of $[L_2V_2O_2(\mu\text{-}CH_3CO_2)_2]I_2$, which crystallizes in the orthorhombic space group $P2_12_12_1$ with $a = 21.665$ (2) Å, $b = 23.301$ (4) Å, $c = 13.161$ (2) Å, and $Z = 8$. It consists of binuclear bis(μ-acetato)-bis(vanadyl(IV)) dications. The terminal oxo groups are syn-positioned with respect to each other, and the nonbonded O···O distance is rather short (2.73 (1) Å), whereas the V···V distance is quite long (4.08 (1) Å). Strong intramolecular antiferromagnetic spin-exchange coupling between the two vanadyl ions (d^1–d^1) is observed ($J = -114$ cm^{-1}; $g = 2.2$). The green complex $[L'_2V_2(\mu\text{-}O)(\mu\text{-}CH_3CO_2)_2]$, where L′ represents the tridentate ligand hydrotripyrazolylborate(1−), has also been prepared; weak ferromagnetic exchange coupling ($J = +5$ cm^{-1}) is observed.

Introduction

Recently we have shown that binuclear metal centers bridged by an oxo group and two carboxylato groups, $[M_2(\mu\text{-}O)(\mu\text{-}CH_3CO_2)_2]$, form readily in aqueous ammonium acetate containing solutions using mononuclear complexes of the type LMX_3 as starting materials.[2a,3] L represents a suitable tridentate N-donor ligand, M has been iron(III)[2] or manganese(III),[3] respectively, and X^- is a unidentate ligand such as chloride or bromide. Studies using the saturated tridentate macrocycle 1,4,7-triazacyclononane[2] or its N-methylated derivative[2-4] and

(1) (a) Ruhr-Universität Bochum. (b) Texas A&M University. (c) Universität Heidelberg.

(2) (a) Wieghardt, K.; Pohl, K.; Gebert, W. *Angew. Chem., Int. Ed. Engl.* **1983**, *22*, 727. (b) Spool, A.; Williams, I. D.; Lippard, S. J. *Inorg. Chem.* **1985**, *24*, 2156.

(3) Wieghardt, K.; Bossek, U.; Ventur, D.; Weiss, J. *J. Chem. Soc., Chem. Commun.* **1985**, 347.

0020-1669/88/1327-0721$01.50/0 © 1988 American Chemical Society